

Triptonide inhibits growth and metastasis in HCC by suppressing EGFR/PI3K/AKT signaling

Hao ZHANG¹, Yingxuan MAO², Xiaomeng ZOU², Jiamei NIU², Jian JIANG², Xi CHEN², Mingwei ZHU², Xiuhua YANG², Tianxiu DONG^{2,*}

¹Department of Medical Imaging, Heilongjiang Provincial Hospital, Harbin, China; ²Department of Abdominal Ultrasound, The First Affiliated Hospital of Harbin Medical University, Harbin, China

*Correspondence: dtx123@163.com

Received November 18, 2022 / Accepted December 16, 2022

Liver cancer represents one of the deadliest cancers, with a rising incidence worldwide. Triptonide is found in the traditional Chinese medicinal plant *Tripterygium wilfordii* Hook. This study aimed to examine the anticancer properties of triptonide in human hepatocellular carcinoma (HCC). HCC cells were administered with triptonide at various levels, and CCK-8 and colony formation assays were carried out for detecting HCC cell proliferation. Then, cell apoptosis and cell cycle distribution were evaluated by flow cytometry. Tumor growth was monitored noninvasively by ultrasound imaging. Cell migration and invasion were quantitated by wound healing and Transwell assays. A metastasis model was established via tail vein injection of HCC cells in nude mice. Immunoblot was performed to quantitate the expression of proteins involved in the EGFR/PI3K/AKT signaling and its downstream effectors. Triptonide repressed cell proliferation and induced cell cycle arrest and apoptosis in cultured HCC cells, and suppressed tumor growth *in vivo*. In addition, triptonide inhibited EMT, migration and invasion in cultured HCC cells, and lung metastasis in nude mice. Mechanistically, triptonide acted by inhibiting the EGFR/PI3K/AKT signaling and regulated its downstream effectors, e.g., the cell cycle-associated protein cyclin D1, the apoptosis-related protein Bcl-2, the EMT marker E-cadherin, and the invasion-related protein MMP-9. Triptonide suppresses proliferation, EMT, migration and invasion, and promotes apoptosis and cell cycle arrest by repressing the EGFR/PI3K/AKT signaling. Therefore, triptonide might be considered for liver cancer treatment.

Key words: triptonide; hepatocellular carcinoma; EGFR; tumor growth; tumor metastasis

Liver cancer represents one of the deadliest cancers, with rising incidence worldwide [1]. For all stages combined, 5-year patient survival in liver cancer is only 20%, i.e., the second lowest among all cancers; hepatocellular carcinomas (HCCs) comprise 75–85% of primary liver cancers [2, 3]. Conventional cancer therapeutic strategies, including surgery, chemotherapy, and radiotherapy, exert unsatisfactory anticancer effects and/or are highly toxic. In addition, most HCC cases have cirrhosis, with diagnosis commonly made at the middle or late stage, leading to a low surgical resection rate [4]. Currently, sorafenib, a multiple tyrosine kinase inhibitor, is widely utilized for treating advanced HCC, but its effectiveness rate is lower than 20% and the survival of HCC patients increases by merely a few months due to severe adverse events and drug resistance [5]. Therefore, developing new and more efficient agents for HCC treatment is imperative.

Natural products attract increasing attention as a rich source for discovering antitumor compounds and have

been applied in alternative medicine for millennia to treat diverse human health conditions. Triptonide (TN) is a small molecule compound with the molecular formula C₂₀H₂₂O₆ and a molecular weight of 358.39 Da, which is produced by the Chinese plant *Tripterygium wilfordii* Hook [6]. TN strongly inhibits many pathological conditions, including inflammation and malignant tumors. A recently published report revealed that TN potently suppresses myeloid leukemia, prostate cancer, pancreatic cancer, lung cancer, and breast cancer cells [7–11]. In human nasopharyngeal carcinoma, TN inhibits tumor cell growth by disrupting lncRNA THOR-IGF2BP1 signaling [12]. In addition, TN suppresses the malignant potential of lung cancer cells by inhibiting Shh-Gli1 signaling [7]. However, TN has not been examined for its effects on HCC progression.

Epidermal growth factor receptor (EGFR) is expressed on cells and interacts with the epidermal growth factor. Abnormal activation of EGFR is associated with a variety of tumors. EGFR expression is high in 40–70% of HCC tissues,

and several reports have shown EGFR promotes tumor cell proliferation and metastasis [13]. E-cadherin/ β -catenin complex destabilization is a way for EGFR activation that alters cell-cell adhesion, by which EGFR promotes EMT progression for a motile phenotype [14].

In this work, we first found that TN inhibited HCC growth and progression. We demonstrated that TN suppressed proliferation, EMT, migration and invasion, and induced apoptosis and cell cycle arrest by repressing the EGFR/PI3K/AKT signaling. This study provides a novel strategy for HCC growth and metastasis inhibition and offers a novel candidate drug for HCC treatment.

Materials and methods

Cells and reagents. HCCLM3 and Huh7 cells were from the Institute of Chinese Academy of Science, China. HepG2 cells were from the American Type Culture Collection (USA). The above HCC cells underwent culture in Dulbecco's modified Eagle's medium (DMEM) containing 10% fetal bovine serum (FBS) and 1% antibiotic cocktail at 37°C with 5% CO₂. Triptonide was provided by Solarbio Science & Technology (China) (The purity was $\geq 98\%$ as assayed with HPLC) and dissolved in DMSO to 5 mM before further dilutions with the medium. The primary antibodies used to detect p-EGFR (#3777), EGFR (#4267), p-AKT (#4060), AKT (#4691), E-cadherin (#3195), N-cadherin (#13116), Vimentin (#5741), and cleaved PARP (#5625) were provided by Cell Signaling Technology (USA). p-PI3K (ab182651) was provided by Abcam (UK). Antibodies targeting Bcl-2 (Cat. No. 12789-1-AP), Cyclin D1 (Cat. No. 60186-1-Ig), and β -actin (Cat. No. 66009-1-Ig) were provided by Proteintech Group (China).

Proliferation assays. For the CCK-8 assay, $2\text{--}5 \times 10^3$ HCC cells/well were seeded in a 96-well plate and incubated with or without TN for 24 h, 48 h, and 72 h. At 1 to 3 days, the CCK-8 solution (Saint-Bio, China) was added as directed by the manufacturer, followed by incubation at 37°C for 2 h. Finally, optical density at 450 nm was read on a spectrophotometer.

Colony formation assay. HCCLM3, HepG2, and Huh7 cells underwent seeding in culture dishes at 0.5×10^3 /dish for a 24 h culture. After culture medium aspiration, fresh medium with different doses of TN was added for further culture at 37°C for 24 h. Then, the supernatants were replaced with 2 ml DMEM with 10% FBS, and the cells were cultured until visible cell colonies were formed. After crystal violet staining, colony count was performed under a light microscope.

Apoptosis assessment. HCC cells were harvested after TN treatment for 48 h. After washing, cells underwent successive incubations with Annexin V-FITC (10 μ l, 15 min) and propidium iodide (PI; 5 μ l, 5 min shielded from light). Next, 400 μ l of PBS was added per sample, and flow cytometry was used to analyze the samples (Beckman Coulter).

Cell cycle assay. HCC cells were administered TN (30 nM) for 48 h and underwent fixation. Subsequently, the cells were submitted to RNase digestion and PI staining, before cell cycle analysis by flow cytometry.

Wound-healing assay. HCC cells seeded in a 6-well plate were cultured to confluence. Then, a 200 μ l pipette tip was utilized for wound generation. Cells were then treated with mitomycin (20 μ g/ml) for 30 min. After 2 PBS washes, they were subsequently incubated with a medium with or without TN. The cells were imaged at 24 h and 48 h with an inverted digital camera.

Transwell assay. Transwell cell migration and invasion assays were carried out in Transwell plates with or without Matrigel-coated membranes (8 μ m) (BD Biosciences, USA). HCC cells (2×10^4) in DMEM with no FBS were added to the superior compartment of a Transwell. DMEM (800 μ l) with 10% FBS was placed in the inferior compartment. The samples were incubated for 48–72 h, and HCC cells on the upper surface of the filters were removed and washed with PBS. Those that traversed the membrane underwent fixation with methanol and staining with 0.5% crystal violet. The migratory and invasive abilities of HCC cells were analyzed by microscopy and expressed as ratios relative to untreated cells. Triplicate assays were performed thrice independently.

Immunoblot. Cell lysis was carried out with RIPA lysis buffer with protease and phosphatase inhibitors. Protein concentration was assessed with the BCA protein assay kit (Beyotime Institute of Biotechnology, China). Total protein underwent separation by SDS-PAGE, followed by electrotransfer onto nitrocellulose membranes (Pall Corporation, USA). After blocking with 5% skimmed milk, each membrane underwent successive incubations with primary (overnight, 4°C) and secondary (1 h at ambient temperature) antibodies. An infrared imaging system (Odyssey NIR, LI-COR, USA) was used for visualization.

Animal studies. Four-to-six-week-old male BALB/c nude mice, purchased from Charles River (China), underwent housing under specific pathogen-free conditions. HCCLM3 cells (4×10^6 /ml, 200 μ l) were administered by subcutaneous injection to the left flank of mice. When tumors reached about 100 mm³, the animals were randomized into two groups: normal saline and TN injection groups (n=4). Corresponding injections (5 mg/kg) were performed every 2 days [7, 15, 16]. Ultrasound imaging, including B-mode imaging and CDFI, was used to monitor tumor growth at 0, 7, and 14 days after TN treatment. A metastasis model was established via tail vein injection of 4×10^6 HCCLM3 cells in nude mice (4 animals/group). At 7 weeks, nude mice were sacrificed, and their lungs were resected and fixed. Animal experiments had approval from the Institutional Animal Care and Use Committee of Harbin Medical University and followed current guidelines.

Statistical analysis. GraphPad Prism 7 (GraphPad Software, USA) and SPSS 16.0 (IBM, USA) were utilized for data analysis. Data are mean \pm standard deviation (SD) and

were compared by the Student's t-test or ANOVA. A p-value <0.05 indicated statistical significance.

Results

TN inhibits proliferation in HCC cells *in vitro*. We first investigated whether TN affects viability in HCC cell lines including HCCLM3, HepG2, and Huh7 cells, and the normal hepatic cell line L02. In this respect, increasing concentrations of TN (0–100 nM) were used to treat HCC cells for 24 h to 72 h, followed by cell viability evaluation with CCK-8 assay. As depicted in Figure 1A, TN inhibited the viability of the 3 HCC cell lines; while an antitumor effect for TN was not notable at 24 h, TN mainly played a role after 48 h. The 50% inhibitory concentrations (IC50s) of TN in HCCLM3, HepG2, and Huh7 cells were about 66.97 nM, 46.63 nM, and 70.58 nM at 48 h, respectively. However, TN had no obvious effect on L02 cells (Figure 1B). Colony formation assays also demonstrated the antiproliferative effect of TN on HCC cells, and the numbers and sizes of colonies gradually decreased with increasing concentrations in all 3 HCC cell lines (Figures 1C, 1D).

TN induces cell cycle arrest and apoptosis in cultured HCC cells. Cell cycle arrest and apoptosis are two main factors that inhibit proliferation; hence, flow cytometry was further applied to evaluate TN's effect on the cell cycle distribution and apoptosis. Statistical analysis indicated that the proportions of apoptotic HCCLM3, HepG2, and Huh7 cells upon TN treatment were elevated in comparison with control cells at 48 h (Figures 2A, 2B). To identify the proteins contributing to apoptosis induction in TN-treated cells, Bcl-2 and cleaved PARP protein amounts were determined by immunoblot.

The amounts of Bcl-2, known as an antiapoptotic factor, were markedly reduced by TN, dose-dependently, while cleaved PARP levels were increased (Figure 2C).

The cell cycle machinery is considered an important diagnostic and therapeutic target in malignancies, and its dysregulation results in abnormal cell division characterizing all cancers [17]. Cell cycle arrest induces apoptotic cell death. Cell cycle assays showed that G1 phase arrest occurred in all three HCC cells upon TN administration, and the cell proportions in the S and G2 phases were reduced. The percentages of HCC cells were elevated in the G1 phase (Figures 2D–2F). Based on the results of flow cytometry analysis, Cyclin D1 was detected by immunoblot. As depicted in Figure 2G, Cyclin D1 protein amounts were decreased after TN treatment, dose-dependently. These results reveal that TN may suppress HCC cell proliferation by arresting cells at the G1 phase. The above findings jointly demonstrated TN inhibits HCC cell proliferation via apoptosis and cell cycle arrest.

TN suppresses HCC tumors *in vivo*. To determine the *in vivo* effect of TN on HCC, nude mice with experimental HCC were administered TN (5 mg/kg) for 14 days. Tumors were monitored noninvasively by ultrasound imaging, including B-mode imaging and CDFI. Tumor sizes were reduced in the TN-treatment group compared with control animals. Blood vessels formed stably in control mice at 14 days, while blood vessel formation was not obvious in TN-treated mice (Figure 3A). After TN treatment completion, subcutaneously transplanted tumors were removed and measured using Vernier calipers. Tumor growth was reduced after TN treatment in comparison with control animals, as reflected by tumor volumes and weights (Figures 3B–3D). To further investigate the *in vivo* antiproliferative effect of TN,

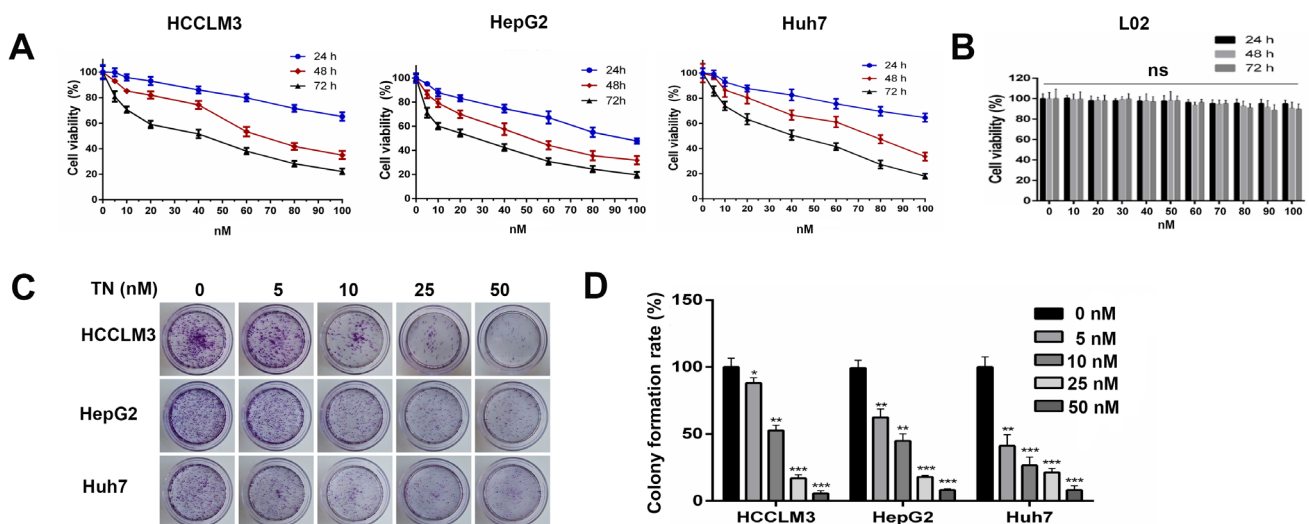


Figure 1. TN inhibits proliferation in cultured HCC cells. A) HCCLM3, HepG2, and Huh7 cell viability was assessed with CCK-8 assay. B) L02 cell viability was assessed with CCK-8 assay. C) Colony formation assay was carried out for assessing TN's suppressive effect on cell proliferation. D) Colony formation rates of HCC cells after treatment with TN. Assays were performed thrice independently. Data are mean \pm SD. *p<0.05, **p<0.01, ***p<0.001 vs. control group

we evaluated the expression of Ki-67, which is a biomarker of cell proliferation, in xenografts by immunohistochemical staining. Ki-67-positive cells were overtly fewer in TN-treated tumors in comparison with control tumors. The TUNEL assay was further carried out to demonstrate TN's effect on apoptosis; indeed, there were more apoptotic cells in TN-treated tumors in comparison with control animals (Figures 3E–3G). Hematoxylin and eosin (H&E) staining demonstrated that TN treatment did not cause obvious necrosis in major organs from mice including the heart, liver, spleen, lung, and kidney (Figure 3H).

TN inhibits migration and invasion abilities in HCC *in vitro* and *in vivo*. To examine TN's effects on cell motility, HCCLM3, HepG2, and Huh7 cells were administered with 20 nM TN. Wound healing assays revealed that TN decreased the cell migration abilities of HCCLM3, HepG2, and Huh7

cells both at 24 h and 48 h (Figures 4A, 4B). Migratory and invasive abilities were also evaluated by Transwell assays without and with Matrigel coating, respectively. As depicted in Figures 4C and 4D, migratory and invasive abilities in these cells were both inhibited in TN treatment groups. In addition, the expression of MMP-9, a critical matrix metalloproteinase, was assessed. Immunoblot revealed MMP-9 expression was decreased dose-dependently. EMT is a pivotal developmental regulatory program that promotes tumor migration and invasion in epithelium-derived carcinomas. Therefore, we then determined whether TN inhibits HCC proliferation, migration, and invasion via EMT. Typical EMT biomarkers, i.e., E-cadherin, N-cadherin, and Vimentin, were examined. As depicted in Figure 4E, E-cadherin protein amounts were elevated, while N-cadherin and Vimentin protein levels were reduced in TN-treated cells. This finding indicated that TN

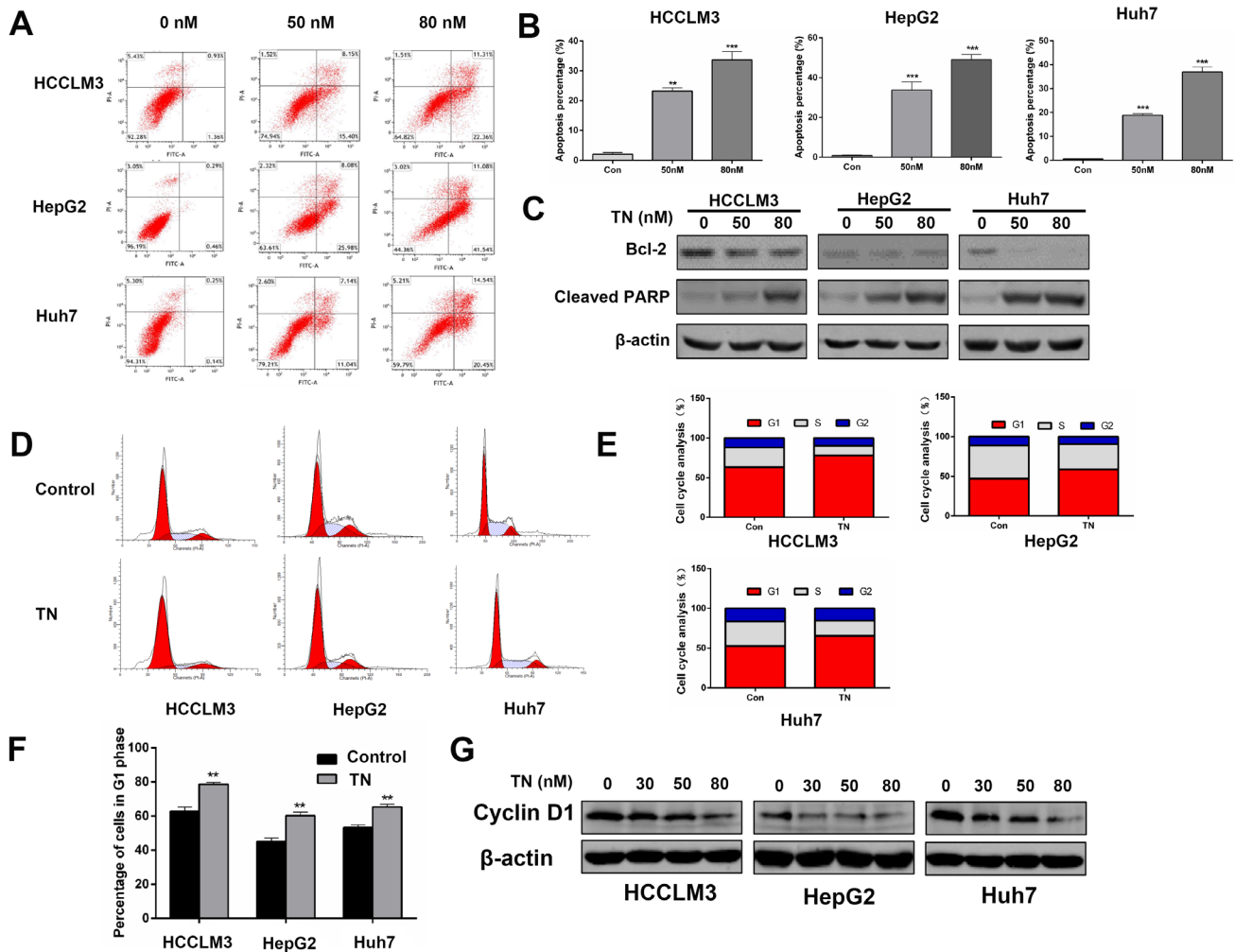


Figure 2. TN induces apoptosis and cell cycle arrest in cultured HCC cells. A) Apoptosis was examined in HCC cells administered TN at various amounts. B) Percentages of apoptotic cells upon TN administration. C) Bcl-2 and cleaved PARP protein amount determined by immunoblot, normalized to β-actin expression. D–F) Flow cytometry assessment of cell cycle distribution in HCC cells administered TN. G) Amounts of cell cycle-associated proteins, determined by immunoblot, normalized to β-actin expression. Assays were performed thrice independently. Data are mean ± SD. **p<0.01, ***p<0.001 vs. control group

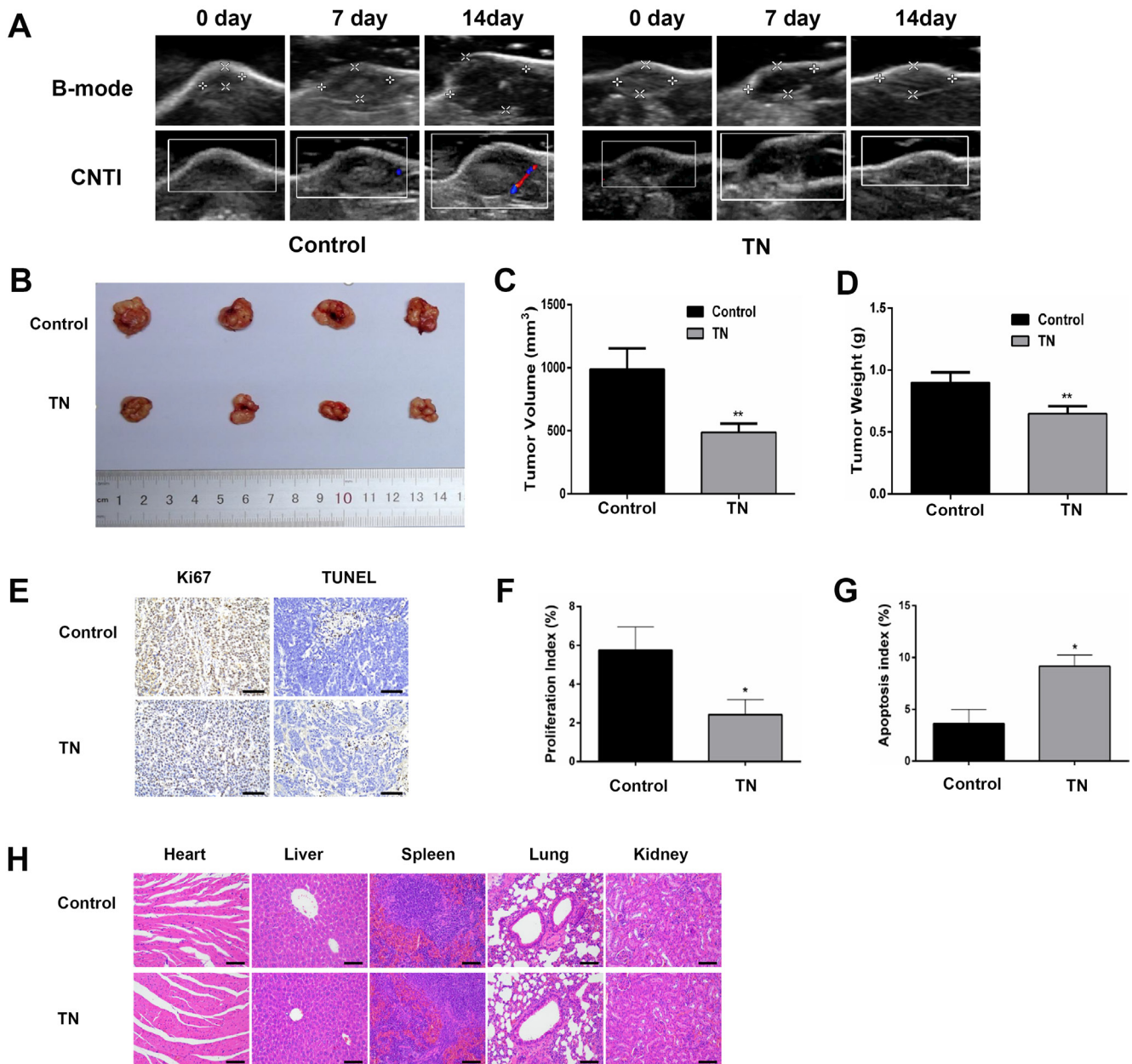


Figure 3. TN inhibits the growth of HCC tumors in mice. HCCLM3 cells were administered by subcutaneous injection into the left flank of the animals. During TN treatments for 2 weeks, all tumors in mice were observed by US (A). B) Photographs of excised tumors at 14 days of treatment. C) Tumor volumes and D) tumor weights were assessed. E) Expression of Ki-67 in xenografts, determined immunohistochemically, and TUNEL assay data (scale bar: 100 μ m). F, G) corresponding statistical results. Assays were performed thrice independently. Assays were performed thrice independently. Data are mean \pm SD. * $p < 0.05$, ** $p < 0.01$ vs. control group. H) H&E staining of the major organs including the heart, liver, spleen, lung, and kidney from tumor-bearing mice treated without/with TN (scale bar: 100 μ m).

repressed HCC cell growth and metastasis through EMT. To further assess TN's effect on metastasis *in vivo*, HCCLM3 cells were administered by tail vein injection into nude mice. After the seventh week of treatment, mice underwent euthanasia, and lungs were extracted. H&E staining revealed fewer and smaller lung metastases after TN treatment in comparison with control animals (Figures 4F, 4G).

TN inhibits HCC by repressing EGFR/PI3K/AKT signaling. Because the EGFR system controls HCC occurrence and progression, we examined the expression of EGFR and its phosphorylated form (p-EGFR) and found p-EGFR expression was downregulated; to some extent, total EGFR was decreased by TN at 80 nM. As a major downstream signaling pathway, PI3K/AKT effectors were

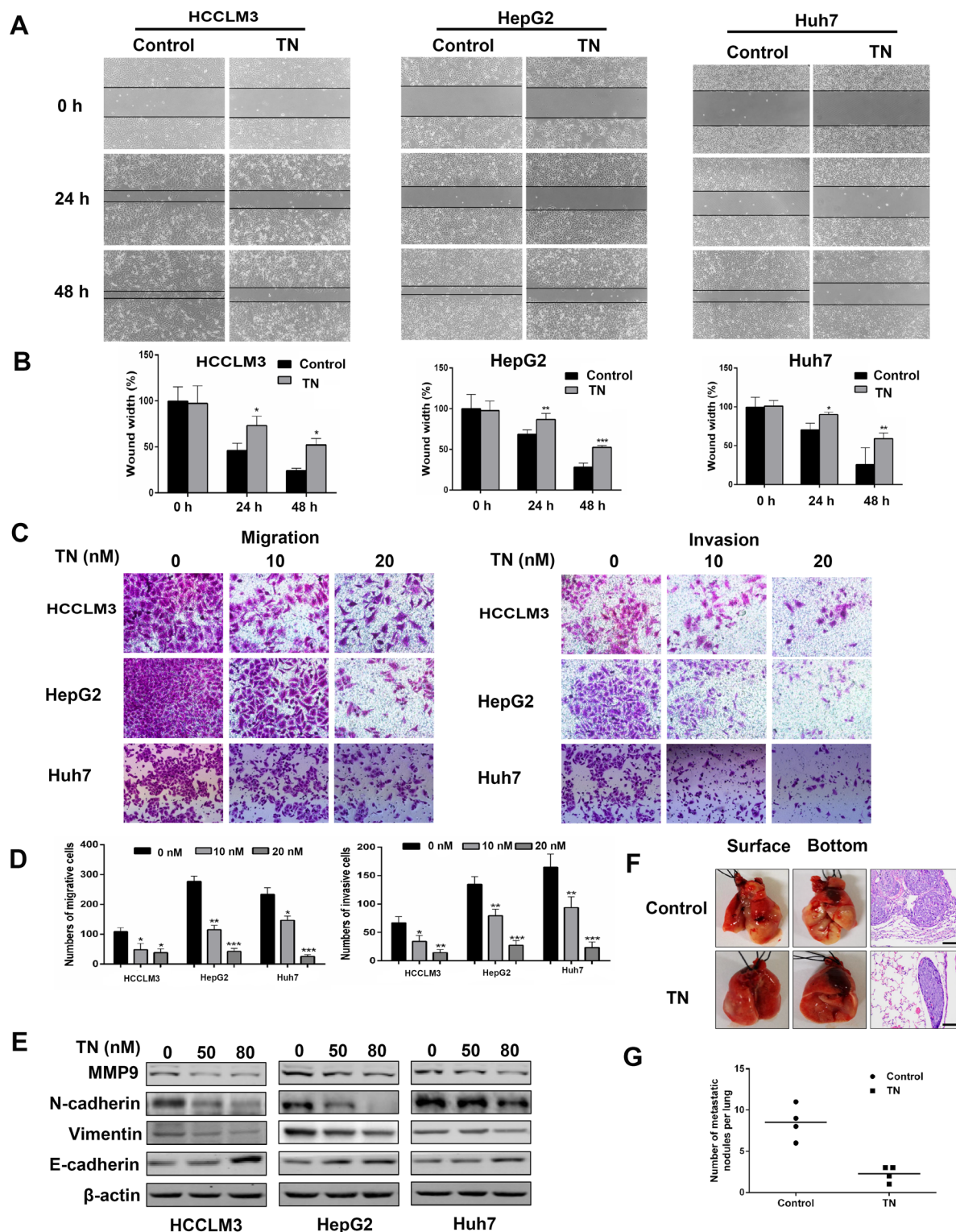


Figure 4. TN suppresses migration and invasion in HCC cells *in vitro* and *in vivo*. A, B) Representative micrographs and quantification of the wound-healing assay for HCC cells of various groups. C, D) Representative micrographs and quantification of HCC cell migration and invasion by Transwell assays. E) MMP-9, E-cadherin, N-cadherin and Vimentin protein amounts examined by immunoblot in HCC cells. F) Holistic view and H&E staining of lungs from the established mouse metastasis model. Representative images of lung tissues are shown in the left panel. The respective H&E staining data of metastatic lung foci are depicted in the right panel. Scale bar = 100 μ m. G) Number of metastatic lung nodules for various groups. Data are mean \pm SD from three experiments performed independently. * p <0.05, ** p <0.01, *** p <0.001 vs. control group

assessed by immunoblot. TN inhibited p-PI3K and p-AKT amounts (Figures 5A, 5B). The above findings indicated TN may inhibit HCC proliferation, migration, and invasion via EGFR/PI3K/AKT signaling suppression.

Discussion

TN represents a phenolic substance that was first reported in *Tripterygium wilfordii* Hook in the early 1990s. TN has been attributed to anti-inflammatory and antitumor properties by previously published reports. It exerts antitumor effects by modulating some tumor-associated signaling pathways. Here, TN decreased viability and induced apoptosis and cell cycle arrest in HCC cells, and inhibited growth and metastasis *in vivo*, at least partly, by suppressing EGFR/PI3K/AKT signaling.

Here, we showed that TN inhibited HCC cell proliferation dose- and time-dependently, with IC₅₀s lower than 100 nM in all examined HCC cells, which were starkly lower than those of sorafenib, a clinically targeted drug used for HCC [18]. Multiple reports have demonstrated cell cycle arrest and apoptosis suppress cell growth [19]. Therefore, we examined whether TN could promote cell cycle arrest or apoptosis in HCC cells. Apoptosis represents a well-controlled cell death type that works by eradicating unnecessary and harmful cells. Interestingly, dysregulated apoptosis promotes tumorigenesis [20, 21]. As shown above, TN promoted apoptosis dose-dependently. In mitochondrial pathway of apoptosis, Bcl-2 family proteins serve as an “apoptotic switch” [22]. Bcl-2 is found in the

mitochondrial outer membrane, where it promotes cell survival and inhibits proapoptotic proteins, and cleaved PARP is a downstream substrate of Bcl-2, representing another indicator of apoptosis [23, 24]. Therefore, we evaluated Bcl-2 and cleaved PARP protein amounts, and altered Bcl-2 and cleaved PARP amounts demonstrated that TN promotes the apoptotic process by affecting the intrinsic apoptotic pathway. The cell cycle machinery is a potential diagnostic and therapeutic target in malignancies since its dysregulation results in abnormal cell division characterizing all cancers. The above flow cytometry results showed that cell cycle arrest occurred at the G1 stage after TN treatment. In addition, consistent results were obtained by the expression alteration of Cyclin D1 assessed by immunoblot. Importantly, TN injection intraperitoneally markedly reduced subcutaneous xenograft growth in mice. The above findings suggest a potent anti-HCC effect for TN.

Metastasis is a process by which malignant cells move from the primary site to other sites or organs far off. EMT is the first event that causes tumor cell detachment from primary tumors and promotes local migration and invasion. Here, we first demonstrated that TN suppressed the invasive and migratory abilities of HCC cells, and found that the EMT markers N-cadherin and Vimentin were downregulated, while E-cadherin was upregulated. MMPs, a family of zinc-containing endopeptidases, control extracellular matrix (ECM) degradation in multiple cell processes of tumor progression such as wound healing, angiogenesis, migration, and invasion. This study showed that the expression of MMP-9 decreased after TN treatment.

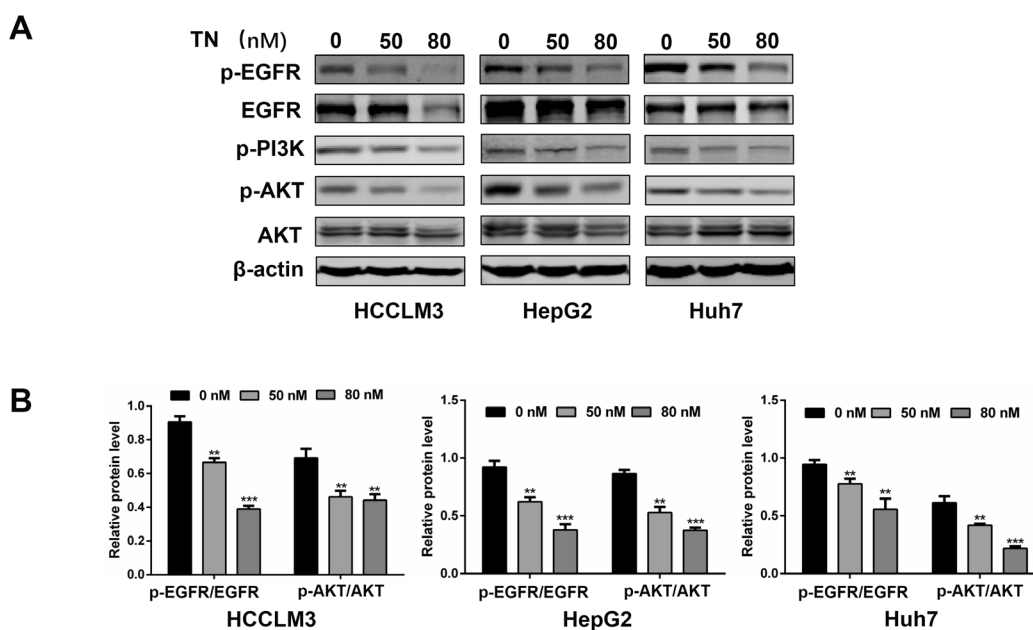


Figure 5. TN inhibits HCC by repressing EGFR/PI3K/AKT signaling. A) Immunoblot assessment of EGFR/PI3K/AKT signaling-associated proteins. B) Immunoreactive bands were assessed for density. Data are mean \pm SD from three experiments performed independently. * $p < 0.05$, ** $p < 0.01$, *** $p < 0.001$ vs. control group

EGFR drives tumorigenesis in multiple malignancies, including HCC, lung cancer, breast cancer, and glioblastoma [25]. The EGFR system is involved in the occurrence of HCC from the early stage of the disease [26]. Activation of EGFR promotes HCC proliferation and differentiation by triggering RAS/MAPK and PI3K/AKT signal transduction cascades. Numerous studies have demonstrated that the EGFR/PI3K/AKT pathway promotes proliferation, EMT, and metastasis [27–29]. EGFR can be activated by chemotherapy in highly proliferative cells, resulting in its translocation into the nucleus; nuclear EGFR is related to cyclin D1, a critical regulator of the transition through the G1 checkpoint during the cell cycle. In addition, EGFR-dependent ERK and AKT induction increases the amounts and activities of MMPs, which are critical regulators of cell migration and invasion. Pei *et al.* also reported that MMP-9 is an EGFR/PI3K/AKT pathway downstream effector [30]. Our results are consistent with these reports, revealing TN suppresses HCC growth and metastasis via EGFR/PI3K/AKT signaling.

These findings suggest TN suppresses proliferation, EMT, migration, and invasion in HCC cells and promotes apoptosis and cell cycle arrest, via inhibition of EGFR/PI3K/AKT signaling and thus regulating its downstream effectors, e.g., the cell cycle-associated protein cyclin D1, the apoptosis-related protein Bcl-2, the EMT marker E-cadherin, and the invasion-related protein MMP-9.

In conclusion, TN suppresses HCC cell proliferation, EMT, migration, and invasion, and promotes apoptosis and cell cycle arrest by repressing EGFR/PI3K/AKT signaling. The above findings indicate TN is a potent candidate drug for HCC therapy.

Acknowledgments: The current study was funded by the Natural Science Foundation of Heilongjiang Province (Grant No. LH2021H068) and the Fund of Scientific Research Innovation of The First Affiliated Hospital of Harbin Medical University (Grant No. 2018B009).

References

- [1] FORNER A, REIG M, BRUIX J. Hepatocellular carcinoma. *Lancet* 2018; 391: 1301–1314. [https://doi.org/10.1016/S0140-6736\(18\)30010-2](https://doi.org/10.1016/S0140-6736(18)30010-2)
- [2] SIEGEL RL, MILLER KD, FUCHS HE, JEMAL A. Cancer Statistics, 2021. *CA Cancer J Clin* 2021; 71: 7–33. <https://doi.org/10.3322/caac.21654>
- [3] BRAY F, FERLAY J, SOERJOMATARAM I, SIEGEL RL, TORRE LA et al. Global cancer statistics. 2018. *GLOBOCAN estimates of incidence and mortality worldwide for 36 cancers in 185 countries. CA Cancer J Clin* 2018; 68: 394–424. <https://doi.org/10.3322/caac.21492>
- [4] GRAF D, VALLBÖHMER D, KNOEFEL WT, KRÖPIL P, ANTOCH G et al. Multimodal treatment of hepatocellular carcinoma. *Eur J Intern Med* 2014; 25: 430–437. <https://doi.org/10.1016/j.ejim.2014.03.001>
- [5] DONG ZR, SUN D, YANG YF, ZHOU W, WU R et al. TM-PRSS4 Drives Angiogenesis in Hepatocellular Carcinoma by Promoting HB-EGF Expression and Proteolytic Cleavage. *Hepatology* 2020; 72: 923–939. <https://doi.org/10.1002/hep.31076>
- [6] DONG F, YANG P, WANG R, SUN W, ZHANG Y et al. Triptonide acts as a novel antiproliferative cancer agent mainly through inhibition of mTOR signaling pathway. *Prostate* 2019; 79: 1284–1293. <https://doi.org/10.1002/pros.23834>
- [7] ZHANG M, TAN S, YU D, ZHAO Z, ZHANG B et al. Triptonide inhibits lung cancer cell tumorigenicity by selectively attenuating the Shh-Gli1 signaling pathway. *Toxicol Appl Pharmacol* 2019; 365: 1–8. <https://doi.org/10.1016/j.taap.2019.01.002>
- [8] PAN Y, MENG M, ZHENG N, CAO Z, YANG P et al. Targeting of multiple senescence-promoting genes and signaling pathways by triptonide induces complete senescence of acute myeloid leukemia cells. *Biochem Pharmacol* 2017; 126: 34–50. <https://doi.org/10.1016/j.bcp.2016.11.024>
- [9] YANG P, DONG F, ZHOU Q. Triptonide acts as a novel potent anti-lymphoma agent with low toxicity mainly through inhibition of proto-oncogene Lyn transcription and suppression of Lyn signal pathway. *Toxicol Lett* 2017; 278: 9–17. <https://doi.org/10.1016/j.toxlet.2017.06.010>
- [10] HAN H, DU L, CAO Z, ZHANG B, ZHOU Q. Triptonide potently suppresses pancreatic cancer cell-mediated vasculogenic mimicry by inhibiting expression of VE-cadherin and chemokine ligand 2 genes. *Eur J Pharmacol* 2018; 818: 593–603. <https://doi.org/10.1016/j.ejphar.2017.11.019>
- [11] GAO B, CHEN J, HAN B, ZHANG X, HAO J et al. Identification of triptonide as a therapeutic agent for triple negative breast cancer treatment. *Sci Rep* 2021; 11: 2408. <https://doi.org/10.1038/s41598-021-82128-0>
- [12] WANG SS, LV Y, XU XC, ZUO Y, SONG Y et al. Triptonide inhibits human nasopharyngeal carcinoma cell growth via disrupting Lnc-RNA THOR-IGF2BP1 signaling. *Cancer Lett* 2019; 443: 13–24. <https://doi.org/10.1016/j.canlet.2018.11.028>
- [13] HU W, ZHENG S, GUO H, DAI B, NI J et al. PLAGL2-EGFR-HIF-1/2alpha signaling loop promotes HCC progression and Erlotinib insensitivity. *Hepatology* 2021; 73: 674–691. <https://doi.org/10.1002/hep.31293>
- [14] CLAPÉRON A, MERGEY M, NGUYEN HO-BOULDOIRES TH, VIGNJEVIC D, WENDUM D et al. EGFR/EGFR axis contributes to the progression of cholangiocarcinoma through the induction of an epithelial-mesenchymal transition. *J Hepatol* 2014; 61: 325–332. <https://doi.org/10.1016/j.jhep.2014.03.033>
- [15] XIANG S, ZHAO Z, ZHANG T, ZHANG B, MENG M et al. Triptonide effectively suppresses gastric tumor growth and metastasis through inhibition of the oncogenic Notch1 and NF-κB signaling pathways. *Toxicol Appl Pharmacol* 2020; 388: 114870. <https://doi.org/10.1016/j.taap.2019.114870>
- [16] TAN S, ZHAO Z, QIAO Y, ZHANG B, ZHANG T et al. Activation of the tumor suppressive Hippo pathway by triptonide as a new strategy to potentially inhibit aggressive melanoma cell metastasis. *Biochem Pharmacol* 2021; 185: 114423. <https://doi.org/10.1016/j.bcp.2021.114423>

- [17] WILLIAMS GH, STOEBER K. The cell cycle and cancer. *J Pathol* 2012; 226: 352–364. <https://doi.org/10.1002/path.3022>
- [18] PEI T, MENG Q, HAN J, SUN H, LI L et al. (-)-Oleocanthal inhibits growth and metastasis by blocking activation of STAT3 in human hepatocellular carcinoma. *Oncotarget* 2016; 7: 43475–43491. <https://doi.org/10.18632/oncotarget.9782>
- [19] HERMOSILLA VE, SALGADO G, RIFFO E, ESCOBAR D, HEPP MI et al. SALL2 represses cyclins D1 and E1 expression and restrains G1/S cell cycle transition and cancer-related phenotypes. *Mol Oncol* 2018; 12: 1026–1046. <https://doi.org/10.1002/1878-0261.12308>
- [20] COTTER TG. Apoptosis and cancer: the genesis of a research field. *Nat Rev Cancer* 2009; 9: 501–507. <https://doi.org/10.1038/nrc2663>
- [21] PLATI J, BUCUR O, KHOSRAVI-FAR R. Apoptotic cell signaling in cancer progression and therapy. *Integr Biol (Camb)* 2011; 3: 279–296. <https://doi.org/10.1039/c0ib00144a>
- [22] ZHANG Y, CHEN S, WEI C, RANKIN GO, YE X et al. Flavonoids from Chinese bayberry leaves induced apoptosis and G1 cell cycle arrest via Erk pathway in ovarian cancer cells. *Eur J Med Chem* 2018; 147: 218–226. <https://doi.org/10.1016/j.ejmech.2018.01.084>
- [23] HSU HY, LIN TY, HU CH, SHU DTF, LU MK. Fucoidan upregulates TLR4/CHOP-mediated caspase-3 and PARP activation to enhance cisplatin-induced cytotoxicity in human lung cancer cells. *Cancer Lett* 2018; 432: 112–120. <https://doi.org/10.1016/j.canlet.2018.05.006>
- [24] ZHOU X, ZHU A, GU X, XIE G. Inhibition of MEK suppresses hepatocellular carcinoma growth through independent MYC and BIM regulation. *Cell Oncol (Dordr)* 2019; 42: 369–380. <https://doi.org/10.1007/s13402-019-00432-4>
- [25] SINGH G, HOSSAIN MM, BHAT AQ, AYAZ MO, BANO N. Identification of a cross-talk between EGFR and Wnt/beta-catenin signaling pathways in HepG2 liver cancer cells. *Cell Signal* 2021; 79: 109885. <https://doi.org/10.1016/j.cell-sig.2020.109885>
- [26] BERASAIN C, AVILA MA. The EGFR signalling system in the liver: from hepatoprotection to hepatocarcinogenesis. *J Gastroenterol* 2014; 49: 9–23. <https://doi.org/10.1007/s00535-013-0907-x>
- [27] ZHENG H, YANG Y, HONG YG, WANG MC, YUAN SX. Tropomodulin 3 modulates EGFR-PI3K-AKT signaling to drive hepatocellular carcinoma metastasis. *Mol Carcinog* 2019; 58: 1897–1907. <https://doi.org/10.1002/mc.23083>
- [28] CHEN Y, CHEN X, DING X, WANG Y. Afatinib, an EGFR inhibitor, decreases EMT and tumorigenesis of Huh7 cells by regulating the ERK/VEGF/MMP9 signaling pathway. *Mol Med Rep* 2019; 20: 3317–3325. <https://doi.org/10.3892/mmr.2019.10562>
- [29] JANG JW, SONG Y, KIM SH, KIM JS, KIM KM. CD133 confers cancer stem-like cell properties by stabilizing EGFR-AKT signaling in hepatocellular carcinoma. *Cancer Lett* 2017; 389: 1–10. <https://doi.org/10.1016/j.canlet.2016.12.023>
- [30] TIEMIN P, FANZHENG M, PENG X, JIHUA H, RUIPENG S et al. MUC13 promotes intrahepatic cholangiocarcinoma progression via EGFR/PI3K/AKT pathways. *J Hepatol* 2020; 72: 761–773. <https://doi.org/10.1016/j.jhep.2019.11.021>